

NASA Technical Memorandum 100792

A Laser Communication Experiment Utilizing the ACT Satellite and an Airborne Laser Transceiver

(NASA-TM-100792) A LASER COMMUNICATION
EXPERIMENT UTILIZING THE ACT SATELLITE AND
AN AIRBORNE LASER TRANSCEIVER (NASA) 26 p
CSCL 20E

N88-18910

Unclas
G3/36 0128906

Charles E. Provencher, Jr. and Rodney L. Spence
Lewis Research Center
Cleveland, Ohio

Prepared for
Optoelectronics and Laser Applications in Science and Engineering
(O-E LASE '88)
sponsored by the Society of Photo-Optical Instrumentation Engineers
Los Angeles, California, January 10-17, 1988



A LASER COMMUNICATION EXPERIMENT UTILIZING THE ACT SATELLITE
AND AN AIRBORNE LASER TRANSCEIVER

Charles E. Provencher, Jr. and Rodney L. Spence
National Aeronautics and Space Administration
Lewis Research Center
Cleveland, Ohio 44135

ABSTRACT

The launch of a laser communication transmitter package into geosynchronous earth orbit onboard the Advanced Communications Technology (ACT) satellite will present an excellent opportunity for the experimental reception of laser communication signals transmitted from a space orbit. The ACTS laser package includes both a heterodyne transmitter (Lincoln Labs design) and a direct detection transmitter (Goddard Space Flight Center design) with both sharing some common optical components. NASA Lewis Research Center's Space Electronics Division is planning to perform a space communication experiment utilizing the GSFC direct detection laser transceiver. The laser receiver will be installed within an aircraft provided with a glass port for the reception of the signal. This paper describes the experiment and the approach to performing such an experiment.

Described are the constraints placed upon the NASA Lewis experiment by the performance parameters of the laser transmitter and by the ACTS spacecraft operations. The conceptual design of the receiving terminal is given; also included is the anticipated performance capability of the detector.

INTRODUCTION

In recent years, the interest in using a modulated laser beam as a spaceborne communications transport medium has been growing steadily as evidenced by the number of technical articles published. What has been lacking has been the opportunity for hands-on experience with such systems. The Advanced Communications Technology Satellite, a project of NASA Lewis Research Center with extensive industry participation, is scheduled for launch in the spring of 1991. It is planned to have on-board a laser communication package. Included in the package will be a heterodyne laser transceiver, a project of Lincoln Labs, and a direct detection laser transceiver, a project of NASA Goddard Space Flight Center. Also included will be an acquisition and tracking system, being implemented by Lincoln Labs. The presence of this laser transmitter and receiver in geosynchronous orbit will offer experimenters a rare opportunity for hands on activities with laser communication systems. It is the current intention of NASA Lewis' Space Electronics Division to perform a series of experiments utilizing the direct detection laser package on ACTS. This paper will describe SED's approach to performing the experiment, and a brief description of the calculations involved.

DESCRIPTION OF ACTS

A current, major project of NASA Lewis is the Advanced Communications Technology Satellite with a launch planned for the Second Quarter of 1991. Much has already been published about ACTS so very brief comments will suffice here. This satellite has on-board many unique technology items such as a matrix switch, a baseband processor, and a multiple beam antenna that produces steerable beams. Also included is an operating communication frequency of 30 GHz for the uplink and 20 GHz for the downlink. A part of the ACTS system is a versatile earth terminal, the High Bit Rate-Link Evaluation Terminal (HBR-LET), to provide maximum flexibility of operations for experimenters. The satellite is intended to be utilized intensely as an experimenters test bed during the first years of its life, and the ACTS project office is actively seeking experimenters.

Another feature which adds considerably to ACTS uniqueness is the presence of a laser communication package on-board the satellite. This device will permit ACTS to be used for combined RF/laser communication experiments, a rare opportunity in space.

The laser communication package for the ACTS is the result of a collaboration between MIT's Lincoln Labs, which has performed the development of a heterodyne laser system as well as the acquisition and tracking technology, and Goddard Space Flight Center (GSFC), which has developed the direct detection portion of the package. The hardware for these items is being produced by aerospace hardware fabricating contractors.

Figure 1 is an illustration of the ACTS system showing the RF communication links and the associated terrestrial system.

Both Lincoln Labs and GSFC are currently planning on utilizing satellite to earth laser links for the initial operation of the laser communications package. In selecting a concept for a laser communication experiment by NASA Lewis' Space Electronics Division, it was decided that another satellite-to-earth link would not add useful data to that planned for by LL and GSFC. Therefore, consideration was given to a spaceborne or airborne laser terminal. An examination of the costs and difficulties of implementing a spaceborne laser experiment led to the decision to perform the experiments with an airborne laser transceiver. Availability of suitable aircraft such as WPAFB's Laser Communications Test Bed (ref. 1) was a deciding factor. Figure 2 shows the links involved, a duplex laser link between spacecraft and aircraft, and the 30/20 GHz RF link between spacecraft and the HBR-LET earth terminal. The 30/20 GHz link can be considered firm as both the satellite and the HBR-LET design and hardware phases are well underway. The lasercom package design and hardware phases are also underway but the severe technical difficulties of this effort are causing a series of adjustments as the program has progressed. Thus, there are uncertainties as to the status and specific parameters of the lasercom final product. Consequently, what is being described in this paper is proposed laser communication experiment, and the link parameters stated here will not necessarily be the final ones. Figure 2 displays what is presently anticipated as the NASA Lewis-SED lasercom experiment at the time when ACTS is launched.

EXPERIMENT DESCRIPTION

NASA Lewis is proposing to do a lasercom experiment using the on-board direct detection equipment developed by GSFC with the acquisition and tracking systems developed by Lincoln Labs. The NASA Lewis lasercom package is currently anticipated to be a transceiver, mounted on an actively stabilized platform in a large transport type aircraft. The aircraft fuselage would need to contain a window of suitable material for transmission of the laser beams into and out of the aircraft. The lasercom package will include a microprocessor which will aim the lasercom optics at the ACTS, the electronics needed to store the received communication bit stream and then initiate its transmission back to the satellite. There will also be equipment for measuring the bit error rate of the incoming bit stream. Figure 3 is a block diagram of the transceiver and its associated equipment.

An experiment data point would be obtained by transmitting a random bit stream of specific rate ranging from 1.72 to 220 Mbps and with a zero BER from the RF earth terminal up to the ACTS. On-board the ACTS, the 30 GHz signal is converted to a laser signal and transmitted from ACTS via the direct detection laser transmitter (after acquisition has occurred and tracking initiated) to the airborne receiver. The incoming signal will have its BER measured and then will be returned to ACTS via a direct detection laser channel, and thence to the RF earth terminal as a 20 GHz signal and again the BER will be measured.

There are two possible options for handling the data stream. One, as just described is to have the original data stream complete the entire circuit, i.e., earth terminal to ACTS, thence to aircraft and return, and then back to earth. This would simulate a communication channel in which the airborne laser transceiver served as a repeater and all incoming errors were retransmitted. However, baseband processing appears to be a future reality, and so for our experiment, baseband processing could be simulated in one sense by not retransmitting errors in the signal arriving at the aircraft, but instead originating a new data stream of zero BER and transmitting this signal to ACTS and then to the earth terminal. Studies have not yet been performed to determine which option should be utilized for the NASA Lewis lasercom experiment. For this paper, it is assumed that the first option will be utilized and that the incoming signal to the airborne transceiver will be retransmitted including its errors. This situation could change, because prior to final design of the experiment, a Phase A type study sponsored by NASA Lewis will be performed to provide an accurate and more complete definition of the experiment.

Although BER measurements would be the prime test result, and is the test parameter that could be the primary determinant in selecting the length of test runs, many other factors would be measured. Parameters concerned with the aircraft velocity and attitude relating to the spacecraft need to be measured, plus information describing the performance of the isolation optical bench upon which the transceiver is mounted. This information will be required in order to achieve acquisition and tracking and to assess how well these systems performed during the test.

In order to verify the link calculations, various losses will need to be measured. This will involve collecting data on atmospheric conditions, both at the aircraft itself and from wide area NOAA observations. Specific details on type and quantity of this data are yet to be determined. Some losses such

as optical losses are intrinsic to the hardware and must be obtained by test measurement after the hardware has been fabricated. However, some items such as laser diode performance and possible loss in performance will be monitored during the life of the lasercom experiment. It is certain that sensors should be built into the transceiver hardware, but it is not yet certain how many and at what specific locations. The next section discusses the required receiver sensitivity, link calculations, and losses and parameters that need to be specified to perform these calculations.

COMMUNICATION SYSTEM ANALYSIS

Sensitivity of ACTS/Airborne Direct Detection Receivers

In this section required receiver sensitivity will be determined for the ACTS and aircraft optical communication receivers. Receiver sensitivity is defined here to be the average signal power that must be incident on the photodetector in order to achieve a given bit error rate (BER). Although sensitivities will be computed only for binary pulse position modulation (BPPM), the equations to be presented can also be used to analyze the general M-ary PPM case.

A model of the direct detection receiver using an avalanche photodiode (APD) is shown in figure 4. Here, the desired optical signal along with background radiation is collected and focused by the receiving optics onto the depletion region of a reverse-biased APD. An optical filter is placed in front of the detector to reduce the amount of background power. Photons incident on the APD with energy greater than or equal to the band gap energy of the detector material are absorbed, thus producing free electron-hole pairs. These primary photocarriers are accelerated by a high electric field that exists in the APD, and they, in turn, generate more photocarriers through impact ionization. Thus an avalanche process occurs within the APD with each primary carrier undergoing a multiplication that is statistical in nature with mean gain G . The signal input to the decision block will have a desired signal component, a background noise component, and noise components due to the photoelectron and amplifier circuitry. These include:

- (1) Quantum or shot noise arising from the random nature of the photon-to-electron conversion process
- (2) Bulk dark current noise arising from the thermal generation of photocarriers in the pn junction of the APD
- (3) Surface dark current noise that is dependent on surface defects, cleanliness, bias voltage, and surface area
- (4) Thermal noise due to the amplifier load resistance
- (5) Avalanche gain noise due to the statistical nature of the avalanche process and the fact that not all photocarriers undergo the same multiplication

The decision block of the receiver employs a MAP (maximum a posteriori) decoding strategy wherein the detector output current is integrated over each PPM time slot, and the slot with the maximum photoelectron count is assumed to

be the one in which the signal pulse was transmitted. Once the position of the pulse within the PPM word has been decided, output of the corresponding data bits is straight-forward.

In general, receiver sensitivity is a function of the PPM order, bit rate, amount of interfering background power, and performance parameters characterizing the APD and its associated receiver circuitry. The steps needed to calculate required sensitivity are outlined below. Equations were developed from information in references 3 to 6 inclusive.

Step 1. The PPM time slot duration (integration period) is calculated from:

$$\tau = \frac{\log_2 M}{MR_B} \text{ sec} \quad (1)$$

where

M PPM order or time slots per word ($\log_2 M$ bits of information are contained in each PPM word)

R_B data rate (bps)

Step 2. The amount of the background power incident on APD is:

$$P_B = \frac{\pi n_R D_R^2 \theta_R^2}{16} \Delta \lambda W(\lambda) \text{ watts} \quad (2)$$

where

n_R receiver optics efficiency

D_R receiver aperture diameter, cm

θ_R planar angle receiver field of view (FOV), rad

$\Delta \lambda$ the receiver filter optical bandwidth, μ

$W(\lambda)$ spectral radiant emittance of background source, $W/cm^2-\mu$

The equation above is for an extended background source that covers the entire receiver FOV. This will always be the case for the background sources considered here, since the background radiation due to "contained" sources such as stars and planets was found to be negligible in comparison to other noise components. Once background power has been calculated, the average number of background counts/sec and counts/slot can be found from:

$$N_B = \frac{\eta_Q P_B}{h\nu} \text{ counts/sec} \quad (3)$$

$$K_B = N_B \tau \text{ background counts/slot} \quad (4)$$

where

h Planck's constant ($6.62\text{e-}34$ J-sec)

ν frequency of radiation, sec^{-1}

nq detector quantum efficiency (photoelectrons/photon)

Table I shows the background count rates for the ACTS/LCS (Laser Communication Subsystem) and AIR direct detection receivers under different background environments. For the AIR receiver aperture size, a value of 30 cm (11.8 in.) was used in the calculation since it represents the maximum diameter of a practical sized telescope to be mounted on the aircraft. These background count rates will be used later on in calculating receiver sensitivities.

Step 3. The mean of the detector thermal noise is zero, and the variance is:

$$K_{th}^2 = \frac{2K_b T_S \tau}{R_L q^2} \text{ counts}^2 \quad (5)$$

where

K_b Boltzmann's constant ($1.38\text{e-}23$ J/K)

T_S receiver equivalent noise temperature, K

R_L detector load resistance, Ω

q electron charge ($1.602\text{e-}19$ coulomb)

Step 4. The primary photoelectron counts/slot due to the APD bulk dark current and surface leakage current are:

$$K_{DCB} = \frac{I_B \tau}{q} \text{ counts/slot} \quad (6)$$

$$K_{DCS} = \frac{I_S \tau}{q} \text{ counts/slot} \quad (7)$$

where

I_B gain dependent bulk dark current, A

I_S gain independent surface dark current, A

Step 5. The APD output can be effectively approximated using Gaussian statistics. Hence, for a time slot with no optical signal pulse, the probability density function describing the number of counts/slot is:

$$f_0(x) = \frac{1}{\sqrt{2\pi}\sigma_0} e^{-\frac{(x-\mu_0)^2}{2\sigma_0^2}} \quad (8)$$

where

$$\mu_0 = G(mK_S + K_B + K_{DCB}) + K_{DCS} \quad (9)$$

$$\sigma_0^2 = G^2 F(mK_S + K_B + K_{DCB}) + K_{DCS} + K_{th}^2 \quad (10)$$

μ_0 mean photoelectron count in a nonsignal slot

σ_0^2 variance of the photoelectron count in nonsignal slot

G APD mean gain

m transmit laser modulation extinction ratio (ratio of intensity of "off" state to intensity in "on" state)

F APD excess noise factor (due to random avalanche gain)

K_S photoelectron count due to the desired signal

Similarly, for a time slot with the optical signal pulse, the density function is:

$$f_1(x) = \frac{1}{\sqrt{2\pi}\sigma_1} e^{-(x-\mu_1)^2/2\sigma_1^2} \quad (11)$$

where

$$\mu_1 = G(K_S + K_B + K_{DCB}) + K_{DCS} \quad (12)$$

$$\sigma_1^2 = G^2 F(K_S + K_B + K_{DCB}) + K_{DCS} + K_{th}^2 \quad (13)$$

μ_1 mean photoelectron count in a signal slot

σ_1^2 variance of the photoelectron count in signal slot

Step 6. Given that there are m time slots in an M -ary PPM word and that only one of the time slots contains the optical signal pulse, the probability of making a correct decision on the PPM word will be equal to the probability that the photoelectron count in the signal slot is greater than the count in any of the remaining $M-1$ nonsignal slots. Thus the probability of choosing the correct word is:

$$\begin{aligned} \text{PWC} &= \int_{-\infty}^{\infty} \frac{1}{\sqrt{2\pi}\sigma_1} e^{-(x-\mu_1)^2/2\sigma_1^2} \left[\int_{-\infty}^x \frac{1}{\sqrt{2\pi}\sigma_0} e^{-(y-\mu_0)^2/2\sigma_0^2} dy \right]^{M-1} dx \\ &= \int_{-\infty}^{\infty} \frac{1}{\sqrt{2\pi}\sigma_1} e^{-(x-\mu_1)^2/2\sigma_1^2} \left[\text{Erf} \left[\frac{x - \mu_0}{\sigma_0} \right] \right]^{M-1} dx \quad (14) \end{aligned}$$

where

Erf(x) "communications" error function defined here as:

$$\text{Erf}(x) = \int_{-\infty}^x \frac{1}{\sqrt{2\pi}} e^{-z^2/2} dz = \text{Prob}(X \leq x) \quad (15)$$

Note that this definition is different from the "statistical" error function defined by:

$$\text{erf}(x) = \int_0^x \frac{2}{\sqrt{\pi}} e^{-z^2} dz \quad (16)$$

The two are related by the equations:

$$\text{Erf}(x) = \frac{1}{2} + \frac{1}{2} \text{erf}\left(\frac{x}{\sqrt{2}}\right) \quad (17)$$

or

$$\text{erf}(x) = 2\text{Erf}(\sqrt{2}x) - 1 \quad (18)$$

Once we have PWC, the average bit error rate can be written as:

$$\text{BER} = \frac{M}{2(M-1)} (1 - \text{PWC}) \quad (19)$$

Step 7. For the case of BPPM ($M = 2$), equation (19) can be rewritten if we define the SNR of the APD-based PPM receiver to be:

$$\text{SNR} = \frac{\mu_1^2 - \mu_0^2}{\sigma_0^2 + \sigma_1^2} \quad (20)$$

Substituting for μ_1 , μ_0 , σ_1 , and σ_0 we have:

$$\text{SNR} = \frac{G^2 K_s^2 (m-1)^2}{G^2 F [K_s (m+1) + 2(K_B + K_{DCB})] + 2(K_{DCS} + K_{th}^2)} \quad (21)$$

Then (19) can be expressed as:

$$\text{BPPM BER} = \frac{1}{2} \text{erfc}\left(\sqrt{\frac{\text{SNR}}{2}}\right) \quad (22)$$

where

$\text{erfc}(x) = 1 - \text{erf}(x)$ is the "statistical" complementary error function

Step 8. Using equation (19) for $M > 2$ or equation (22) for $M = 2$, let K_s , the desired signal counts/pulse, vary and compute the resulting BER for the given data rate, background power, and APD parameters. The required K_s to achieve a desired BER can then be determined. Once the target K_s is known, the target signal counts/bit, photons/bit, and photons/sec can be found from:

$$C_s = \frac{K_s}{\log_2 M} \text{ counts/bit} \quad (23)$$

$$P_s = \frac{C_s}{\eta_Q} \text{ photons/bit} \quad (24)$$

$$\lambda_s = P_s R_B \text{ photons/sec} \quad (25)$$

Finally, the required average signal power that must be incident on the APD to achieve the desired BER is simply given by:

$$P_R = \lambda_s h\nu \text{ watts} \quad (26)$$

This is, by definition, the required receiver sensitivity. The difference between the actual received power and this required power is the link margin.

Using the steps outlined above, plots of BPPM BER as a function of required signal counts/bit were constructed for the ACT/LCS and AIR direct detection receivers under different background operating conditions (figs. 5 to 8). Since specific parameters describing the DDLT (Direct Detection Laser Transceiver) Si-APD on the ACTS were not available at the time of this writing, typical values for a commercially available device were assumed. These are shown in table II. This same set of APD parameters was also used for the AIR APD. Curves were generated for each of the data rates at which the laser links might operate. From the curves, one observes that, for a particular BER, fewer signal counts/bit are required as the data rate increases. This is due to the fact that at higher data rates, slot times are narrower and less thermal, background, and dark current noise counts occur within each slot; hence, fewer signal counts/slot are needed to maintain the same BER. What is not evident from the plots is that higher peak laser power is required to maintain the same signal counts/slot as data rate increases. For example, doubling the data rate cuts the slot interval by half, and thus to maintain the same signal counts/slot required twice the peak power.

Table III is a summary of the plot information showing the required signal counts/bit and corresponding required power (in dBW) for error rates of $10e-3$, $10e-6$, and $10e-8$. It can be seen that communication with the airborne terminal with the sun in its receive FOV is impractical. Also, the presence of a dark earth in the ACTS FOV introduces negligible background radiation. The required powers shown in the table will be used in the next section for calculating link margins.

Communications Link Analysis

In this section, actual receive power will be calculated for both the forward link (ACTS-to-AIR) and return link (AIR-to-ACTS) and compared with

required power to estimate the amount of link margin at the various data rates with different airborne terminal aperture sizes.

$$P_R = P_T \eta_T \eta_R G_T G_R L_p \left[\frac{\lambda}{4\pi Z} \right]^2 L_A L_{OTHER} \text{ watts} \quad (27)$$

where

P_R	average received power, W
P_T	average transmitted power, W
η_T	transmit optics efficiency
η_R	receive optics efficiency
G_T	gain of the transmitter optics
G_R	gain of the receiver optics
L_p	pointing loss
Z	range
λ	wavelength of source
L_A	atmospheric loss
L_{OTHER}	other losses such as source laser beam combining loss, secondary mirror obscuration losses (in Cassegrainian telescopes), and communication/tracking power split losses

The transmit and receive optics gains can be related to their aperture size and wavelength by:

$$G_T = \left[\frac{D_T \pi}{\lambda} \right]^2 = \frac{4\pi}{\Omega_T} \text{ numeric gain} \quad (28)$$

and

$$G_R = \left[\frac{D_R \pi}{\lambda} \right]^2 = \frac{4\pi}{\Omega_R} \text{ numeric gain} \quad (29)$$

where

D_T	transmit aperture diameter, m
D_R	receive aperture diameter, m
Ω_T	solid angle into which the xmit signal is radiated, sr
Ω_R	solid angle into which the recv signal is concentrated, sr

The pointing loss associated with an angular pointing error, θ , from xmit/recv line-of-sight (LOS) is given by:

$$L_p = \left[\frac{2J_1(\pi\theta D/\lambda)}{\pi\theta D/\lambda} \right]^2 \quad (30)$$

where

L_p xmit/recv pointing loss (numeric)

θ xmit/recv angular pointing error, rad

J_1 () denotes the first order Bessel function

D xmit/recv aperture diameter, m

Received power can then be converted to received signal counts/bit by:

$$C_S = P_R \frac{\eta_Q}{R_B h\nu} \text{ counts/bit} \quad (31)$$

Using the equations above and the link parameters shown in table IV for the ACTS-to-AIR and AIR-to-ACTS links, a parametric analysis was performed to determine the effect of aircraft aperture size on the link performance. Figure 9 shows a plot of received signal counts/bit versus aircraft aperture diameter for the forward ACTS-to-AIR link. A single CW 30 mW laser is assumed to be operating on the ACTS with transmission through a 20 cm (7.9 in.) aperture. Figure 10 shows a similar plot for the return AIR-to-ACTS link with a single CW 50 mW laser source aboard the aircraft.

Table V shows received counts/bit and received average power (dbW) for aircraft aperture sizes of 10, 15, 20, 25, and 30 cm (3.9, 5.9, 7.9, 9.8, and 11.8 in.). By comparing the actual received power (or signal counts/bit) shown in table V with the required power (or signal counts/bit) shown in table III, the amount of margin obtainable for various combinations of BER, data rate, background environment, and aircraft aperture size can be determined. This is shown in table VI, where each of the link margin entries was calculated by subtracting the required power (for the BER, data rate, and background condition in question) from the corresponding actual received power listed in table V. From the link margin table, it is apparent that the forward ACTS-to-AIRCRAFT link is the more constraining of the two. Also, substantially greater margins can be realized if communications occur at night when the amount of interfering background radiation is reduced. In almost all cases, the performance of the forward link at the maximum data rate of 220 Mbps is unacceptable using the single 30 mW GaAs laser planned on the ACTS. In fact, the only condition that yields a margin greater than 3 db at 220 Mbps is a 30 cm aperture on the aircraft and 10⁻³ BER. For optics size in the range of 15 to 20 cm and 10⁻⁶ BER, operation at 27.5 Mbps gives only about 2 to 5 db of margin on the ACTS-to-AIR link. If the data rate is reduced to 1.72 Mbps, then 10 to 12 db margin is available.

To increase the amount of margin on the forward link at the higher data rates, receiver sensitivities were recomputed using a lower noise APD on the aircraft. This APD was assumed to have an effective hole-electron ionization

ratio (k_{eff}) of 0.007, representative of developmental silicon devices. In addition, for a given desired signal count K_S , APD gain was computed to maximize the detector SNR in equation (21). Optimum gain can be found by differentiating equation (21) with respect to G , setting the result equal to zero, and solving for G . By using the fact that the excess noise factor F is related to the APD gain G and hole-electron ionization ratio k_{eff} by,

$$F = k_{eff}G + (1 - k_{eff})\left(2 - \frac{1}{G}\right) \quad (32)$$

the optimum APD gain can be approximated by,

$$G_{opt} = \left[\frac{8K_b T_s}{R_L q^2 k_{eff} K_S} \right]^{1/3}, \quad K_{DCS} \quad \text{and} \quad K_{DCB} \ll K_{th}^2 \quad (33)$$

$K_B \ll K_S$

Table VII shows a comparison of the aircraft receiver sensitivity between the lower noise, optimum gain APD and the APD used earlier (no background radiation is present). Unfortunately, even with the lower noise APD, detection sensitivity is improved by less than 0.5 db for 10-6 BER at 55, 110, or 220 Mbps. Signal shot noise and avalanche gain noise limits the SNR at these higher data rates. Thus, a higher output laser (or laser beam combining) is required on the ACTS to improve the link margin.

ACQUISITION

For the ACTS/AIRCRAFT lasercom experiment, it is not necessary for NASA Lewis to develop an acquisition procedure, as this procedure has been established by the design of the laser communication package on-board ACTS. The acquisition hardware and software is currently being designed and implemented by MIT's Lincoln Labs as part of their heterodyne lasercom effort. Thus, experiments such as the NASA Lewis ACTS to aircraft laser link need only to implement an acquisition system compatible with that on the ACTS. LL as the originator of this design will report on their effort as appropriate. It is sufficient here to give a brief description of the anticipated acquisition procedure sequence.

Acquisition will occur as follows:

(1) First, each terminal, ACTS and the aircraft, must receive location data for the other terminal and then generate a "most probable direction" for aiming their acquisition optics.

(2) The satellite transmits an acquisition beacon, spread out to a 1 mrad beamwidth.

(3) If the "most probable direction" has been sufficiently accurate, the airborne terminal will acquire the ACTS beacon and then transmit a beam of its own back to the satellite. If acquisition does not occur on the first attempt, the 1 mrad beam is moved to other locations adjacent to the initial "most probable" until acquisition does occur.

(4) The ACTS detector acquires the beacon from the airborne unit, and after this has occurred, both laser packages perform the internal adjustments necessary for initiation of fine tracking.

(5) The airborne terminal must continue to transmit its beacon in order that ACTS can maintain tracking of the aircraft. Once communication is initiated, the ACTS beam is reduced to a beamwidth of 4 mrad.

Reference 2 describes a suitable acquisition array, gives it characteristics, and includes acquisition link calculations that are based on these characteristics.

CONCLUSIONS

The calculations described above indicate that even with the constraint of the 30 mW output power of the ACTS direct detection laser transmitter, judicious choice of aperture size, aircraft receiver, and data rate makes feasible an ACTS to aircraft direct detection laser communication experiment. Acquisition and tracking issues have not been addressed in this paper but work performed at Lincoln Labs, Goddard Space Flight Center, and Wright-Patterson AFB indicate that this is also feasible. At the time of this writing, sufficient details about the ACTS laser communication package are not known, so a more specific experiment plan and hardware definition than that presented herein cannot yet be developed. The follow-on effort to this paper will be to resolve specific design details of the airborne transceiver as the definition of the ACTS laser communication package becomes final.

REFERENCES

1. R.J. Feldman, "Feasibility Analysis of An Air-to-Satellite Laser Communications Link," in National Aerospace Electronics Conference, Vol. 3 pp. 1102-1109, 1987.
2. "Preliminary Execution Phase Project Plan Laser Intersatellite Link Advanced Communications Technology Spacecraft," Goddard Space Flight Center, Greenbelt, MD, Aug. 1985.
3. G. Keiser, Optical Fiber Communications, pp. 145-167, McGraw-Hill, New York (1983).
4. J.B. Abshire, "Performance of OOK and Low-Order PPM Modulations in Optical Communications When Using APD-Based Receivers," IEEE Trans. Commun., Com-32 (10), 1140 (1984).
5. C.C. Chen, and C.S. Gardner, "Comparison of Direct and Heterodyne Optical Intersatellite Communication Links," NASA CR-180210, 1987.
6. R.M. Gagliardi and G. Prati, "On Gaussian Error Probabilities in Optical Receivers," IEEE Trans. Commun., Com-28 (9) 1742 (1980).
7. M.J. Windmiller, "Unique Bit-Error-Rate Measurement System for Satellite Communication Systems," NASA TP-2699, 1987.

Table 1. Receiver Background Count Rates for Selected Sources in the FOV

		RADIANCE WATTS 2 CM-MICRON	RECV OPTICS EFFICIENCY	RECV OPTICS SIZE (CM)	RECV FOV (MICRORADS)	OPTICAL FILTER BW (MICRONS)	WAVELENGTH (MICRONS)	QUANTUM EFF	BACKGROUND POWER (WATTS)	BACKGROUND COUNT RATE (COUNTS/SEC)
AIRCRAFT RECV	SUNLIT SKY IN FOV	20	35%	30	100	2.0E-3	.870	70%	2.47E-8	7.6E10
	SUN IN FOV	2000	35%	30	100	2.0E-3	.870	70%	2.47E-6	7.6E12
	MOON IN FOV	3.0E-3	35%	30	100	2.0E-3	.870	70%	3.71E-12	1.1E7
ACTS RECV	SUNLIT CLOUD COVERED EARTH	1.0E-1	60%	20	100	1.6E-2	.840	70%	7.53E-10	2.2E9
	SUNLIT CLEAR EARTH	1.0E-2	60%	20	100	1.6E-2	.840	70%	7.53E-11	2.2E8
	DARK EARTH	1.0E-3	60%	20	100	1.6E-2	.840	70%	7.53E-12	2.2E7

Table 2. Typical Si-APD Based Direct Detection Receiver Parameters

QUANTUM EFFICIENCY	η_q	70%
EFFECTIVE HOLE-TO-ELECTRON IONIZATION RATIO	k_{eff}	0.01
AVERAGE DETECTOR GAIN	G	150
EXCESS NOISE FACTOR	F	3.5
GAIN DEPENDENT BULK LEAKAGE CURRENT	I_B	0.1 nA
GAIN INDEPENDENT SURFACE LEAKAGE CURRENT	I_S	10.0 nA
EQUIVALENT NOISE TEMPERATURE	T_S	400°K
LOAD RESISTANCE	R_L	2000 Ω

Table 3. Required Sensitivities for Aircraft and ACTS Receivers

SIGNAL COUNTS/BIT REQUIRED POWER (dBW)		10-3 BER					10-6 BER					10-8 BER				
		DATA RATE Mbps					DATA RATE Mbps					DATA RATE Mbps				
		1.72	27.5	55	110	220	1.72	27.5	55	110	220	1.72	27.5	55	110	220
AIRCRAFT RECV SENSITIVITY	NO BACKGROUND RADIATION	290	90	70	60	50	460	160	130	110	100	560	200	170	150	140
		-97.88	-90.93	-89.00	-86.67	-84.45	-95.88	-88.43	-86.32	-84.04	-81.44	-95.03	-87.46	-85.15	-82.69	-79.98
	SUNLIT SKY IN RECV FOV	1310	350	250	170	130	2050	550	390	290	230	2430	650	490	370	290
		-91.33	-85.03	-83.48	-82.14	-80.30	-89.39	-83.07	-81.55	-79.83	-77.82	-88.65	-82.34	-80.56	-78.77	-76.81
	SUN IN RECV FOV	12700	3200	2270	1610	1140	19600	4940	3510	2490	1770	23200	5850	4150	2950	2110
		-81.47	-75.42	-73.90	-72.38	-70.87	-79.59	-73.53	-72.00	-70.49	-68.96	-78.85	-72.80	-71.28	-69.75	-68.19
ACTS/ACS SENSITIVITY	NO BACKGROUND RADIATION	290	90	70	60	50	460	160	130	110	100	560	200	170	150	140
		-97.73	-90.77	-88.86	-86.52	-84.29	-95.73	-88.28	-86.17	-83.88	-81.29	-94.87	-87.31	-85.00	-82.54	-79.83
	DARK EARTH IN RECV FOV	290	90	70	60	50	460	160	130	110	100	560	200	170	150	140
		-97.73	-90.77	-88.86	-86.52	-84.30	-95.73	-88.28	-86.17	-83.88	-81.29	-94.87	-87.31	-85.00	-82.54	-79.83
	SUNLIT EARTH IN RECV FOV	360	110	80	60	50	580	180	150	120	110	690	230	190	160	150
		-96.79	-89.90	-88.28	-86.52	-84.30	-94.72	-87.76	-85.55	-83.50	-80.87	-93.97	-86.70	-84.52	-82.25	-79.53

Table 4. ACTS/Aircraft Communication Link Parameters

PARAMETER	ACTS-TO-AIRCRAFT		AIRCRAFT-TO-ACTS	
DATA RATES	1.72, 27.5, 55, 110, AND 220 MBPS		1.72, 27.5, 55, 110, AND 220 MBPS	
MODULATION FORMAT	DIRECT DETECTION BPPM		DIRECT DETECTION BPPM	
SOURCE WAVELENGTH	.870 MICRON		.840 MICRON	
DETECTOR QUANTUM EFF	SI - APD 70%		SI - APD 70%	
AVG XMIT LASER POWER	SINGLE 30mW GaAs laser	-15.23 dbW	SINGLE 50mW GaAs laser	-13.01 dbW
XMIT OPTICS EFFICIENCY	40%	-3.98 db	40%	-3.98 db
XMIT DIAMETER AND GAIN	20 cm APERTURE	117.17 db	PARAMETER TO BE VARIED	
POINTING LOSS	0.5 microrad rms pointing error	-1.02 db	0.5 microrad rms pointing error	-1.02 db
ATMOSPHERIC LOSS CLEAR AIR	0.83	-0.8 db	0.83	-0.8 db
RANGE/SPACE LOSS	38070 km	-294.81 db	38070 km	-295.11 db
RECV OPTICS EFFICIENCY	62%	-2.08 db	62%	-2.08 db
RECV DIAMETER AND GAIN	PARAMETER TO BE VARIED		20 cm APERTURE	117.48 db

Table 5. ACTS/Aircraft Received Power and Signal Counts/Bit vs Aperture Size

		AIRCRAFT OPTICS APERTURE DIAMETER (CM)				
		10 CM	15 CM	20 CM	25 CM	30 CM
ACTS-TO-AIRCRAFT	AVG RECV POWER (dbW)	-89.58	-86.06	-83.56	-81.63	-80.04
	1.72	1960	4410	7841	12251	17642
	27.5	122	276	490	766	1103
	55	61	138	245	383	552
	110	31	69	123	192	276
	220	15	34	61	96	138
AIRCRAFT-TO-ACTS	AVG RECV POWER (dbW)	-87.06	-83.54	-81.04	-79.10	-77.52
	1.72	3384	7614	13535	21149	30455
	27.5	212	476	847	1323	1905
	55	106	238	423	661	952
	110	53	119	212	331	476
	220	26	60	106	165	238

ORIGINAL PAGE IS
OF POOR QUALITY

Table 6. Available ACTS/Aircraft Link Margins

MARGIN (dbW)			10-3 BER					10E-6 BER					10E-8 BER					
			AIRCRAFT APERTURE SIZE (CM)					AIRCRAFT APERTURE SIZE (CM)					AIRCRAFT APERTURE SIZE (CM)					
			10	15	20	25	30	10	15	20	25	30	10	15	20	25	30	
DAYTIME OPERATION (SUNLIT SKY IN AIR RECV FOV SUNLIT EARTH IN ACTS RECV FOV)	AIRCRAFT-TO-AIRCRAFT	DATA RATE (MBPS)	1.72	1.75	5.27	7.77	9.70	11.29	-0.19	3.33	5.83	7.76	9.35	-0.93	2.59	5.09	7.02	8.61
		27.5	-4.55	-1.03	1.47	3.40	4.99	-6.51	-2.99	-0.49	1.44	3.03	-7.24	-3.72	-1.22	0.71	2.30	
		55	-6.10	-2.58	-0.08	1.85	3.44	-8.03	-4.51	-2.01	-0.08	1.51	-9.02	-5.50	-3.00	-1.07	0.52	
		110	-7.44	-3.92	-1.42	0.51	2.10	-9.75	-6.23	-3.73	-1.80	-0.21	-10.81	-7.29	-4.79	-2.86	-1.27	
		220	-9.28	-5.76	-3.26	-1.33	0.26	-11.76	-8.24	-5.74	-3.81	-2.22	-12.77	-9.25	-6.75	-4.82	-3.23	
	AIRCRAFT-TO-ACTS	DATA RATE (MBPS)	1.72	9.73	13.25	15.75	17.69	19.27	7.66	11.18	13.68	15.62	17.20	6.91	10.43	12.93	14.87	16.45
		27.5	2.84	6.36	8.86	10.80	12.38	3.70	4.22	6.72	8.66	10.24	-0.36	3.16	5.66	7.50	9.18	
		55	1.22	4.74	7.24	9.18	10.76	-1.51	2.01	4.51	6.45	8.03	-2.54	0.98	3.48	5.42	7.00	
		110	-0.54	2.98	5.48	7.42	9.00	-3.56	-0.04	2.46	4.40	5.98	-4.81	-1.29	1.21	3.15	4.73	
		220	-2.76	0.76	3.26	5.20	6.78	-6.19	-2.67	-0.17	1.77	3.35	-7.53	-4.01	-1.51	0.43	2.01	
NIGHTTIME OPERATION (NO BACKGROUND IN AIR RECV FOV DARK EARTH IN ACTS RECV FOV)	AIRCRAFT-TO-AIRCRAFT	DATA RATE (MBPS)	1.72	8.30	11.82	14.32	16.25	17.84	6.30	9.82	12.32	14.25	15.84	5.45	8.97	11.47	13.40	14.99
		27.5	1.35	4.87	7.37	9.30	10.89	-1.15	2.37	4.87	6.80	8.39	-2.12	1.40	3.90	5.83	7.42	
		55	-0.58	2.94	5.44	7.37	8.96	-3.26	0.26	2.76	4.69	6.28	-4.43	-0.91	1.59	3.52	5.11	
		110	-2.91	0.61	3.11	5.04	6.63	-5.54	-2.02	0.48	2.41	4.00	-6.89	-3.37	-0.87	1.06	2.65	
		220	-5.13	-1.61	0.89	2.82	4.41	-8.14	-4.62	-2.12	-0.19	1.40	-9.60	-6.08	-3.58	-1.65	-0.06	
	AIRCRAFT-TO-ACTS	DATA RATE (MBPS)	1.72	10.67	14.19	16.69	18.63	20.21	8.67	12.19	14.69	16.63	18.21	7.81	11.33	13.83	15.77	17.35
		27.5	3.71	7.23	9.73	11.67	13.25	1.22	4.74	7.24	9.18	10.76	0.25	3.77	6.27	8.21	9.79	
		55	1.80	5.32	7.82	9.76	11.34	-0.89	2.63	5.13	7.07	8.65	-2.06	1.46	3.96	5.90	7.48	
		110	-0.54	2.98	5.48	7.42	9.00	-3.18	0.34	2.84	4.78	6.36	-4.52	-1.00	1.50	3.44	5.02	
		220	-2.76	0.76	3.26	5.20	6.78	-5.77	-2.25	0.25	2.19	3.77	-7.23	-3.71	-1.21	0.73	2.31	

TABLE 7. AIRCRAFT RECEIVER SENSITIVITIES WITH TWO DIFFERENT APD'S

AIRCRAFT RECV SENSITIVITY		10-3					10-6					10-8				
		DATA RATE (Mbps)					DATA RATE (Mbps)					DATA RATE (Mbps)				
		1.72	27.5	55	110	220	1.72	27.5	55	110	220	1.72	27.5	55	110	220
		1.72	27.5	55	110	220	1.72	27.5	55	110	220	1.72	27.5	55	110	220
FIRST APD $G=150$ $K_{eff}=0.1$	POWER (dBm)	290	90	70	60	50	460	160	130	110	100	560	200	170	150	140
	COUNTS/ BT	-97.88	-90.93	-89.00	-86.67	-84.45	-95.88	-88.43	-86.32	-84.04	-81.44	-95.03	-87.46	-85.15	-82.69	-79.98
	OPT	563	314	265	222	184	478	254	212	175	144	446	233	194	160	131
LOWER NOISE APD WITH OPTIMAL GAIN AND $K_{eff}=0.007$	POWER (dBm)	200	72	60	51	45	328	136	117	104	93	402	176	154	137	124
	COUNTS/ BT	-99.50	-91.91	-89.68	-87.37	-84.91	-97.30	-89.11	-86.78	-84.28	-81.75	-96.51	-88.01	-85.58	-83.08	-80.50
	OPT	563	314	265	222	184	478	254	212	175	144	446	233	194	160	131

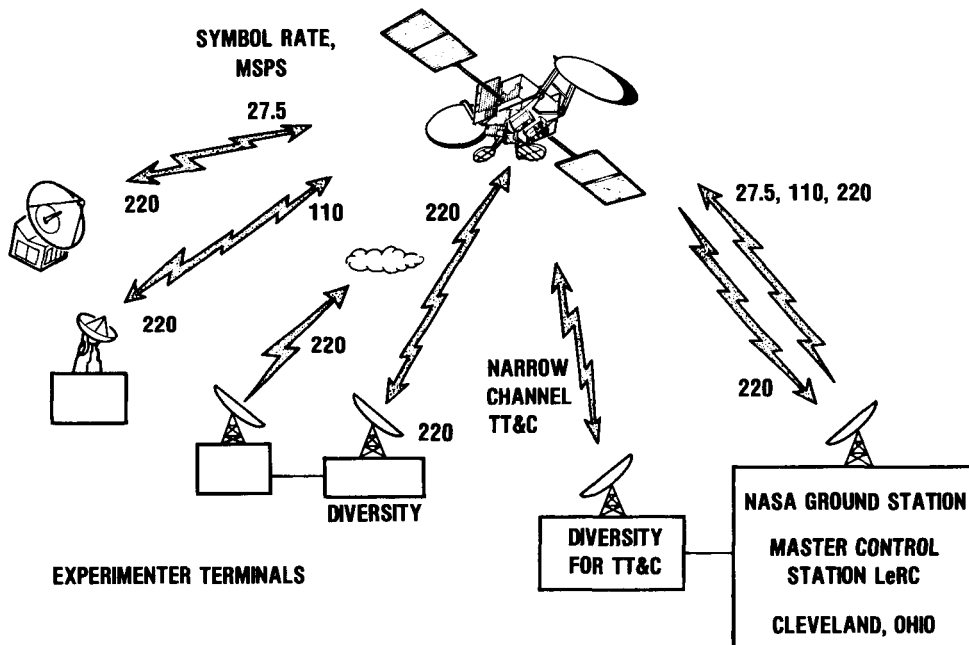


FIGURE 1. - ADVANCED COMMUNICATIONS TECHNOLOGY SATELLITE SYSTEM.

CD-84-15055

ORIGINAL PAGE IS
OF POOR QUALITY

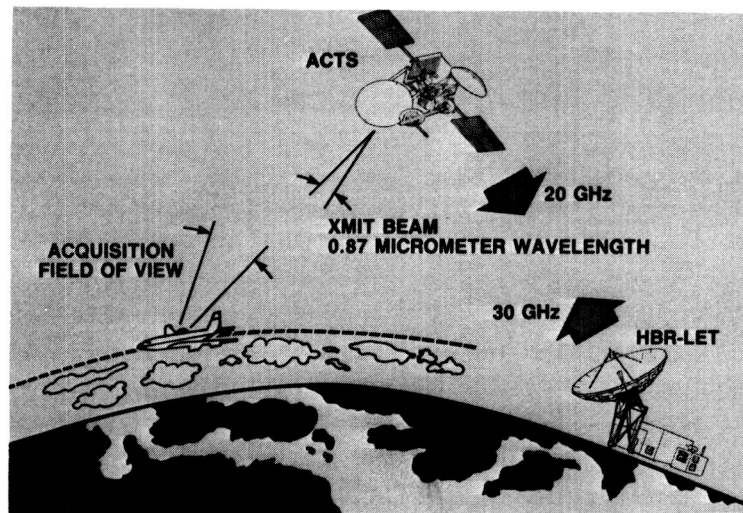


FIGURE 2. - LERC PROPOSED DIRECT DETECTION LASERCOM EXPERIMENT.

ORIGINAL PAGE IS
OF POOR QUALITY

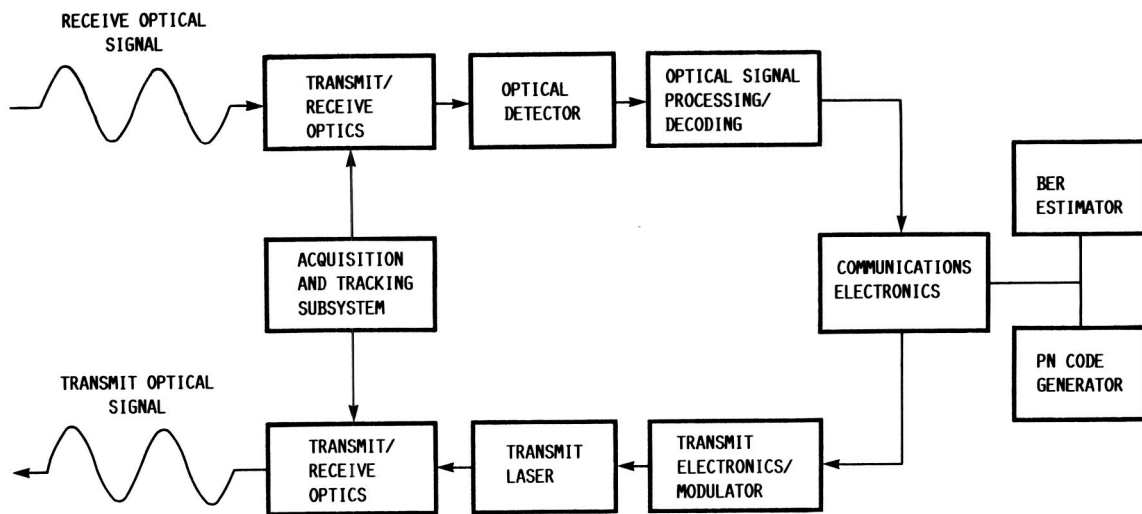


FIGURE 3. - AIRBORNE LASER TRANSCEIVER FUNCTIONAL BLOCK DIAGRAM.

LINK PARAMETERS	
PPM ORDER	M
BIT RATE	R_B
WAVELENGTH	λ
TRANSMIT MODULATION EXTINCTION RATIO	m
TRANSMIT POWER	P_T
OPTICS EFFICIENCY	η_T
APERTURE DIAMETER	D_T
RANGE	Z
POINTING LOSSES	L_P
ATMOSPHERIC AND OTHER LOSSES	L_{OTHER}

RECV OPTICS PARAMETERS	
APERATURE DIAMETER	D_R
PLANAR ANGLE FOV	θ_R
OPTICS EFFICIENCY	η_R
OPTICAL FILTER BANDWIDTH	$\Delta\lambda$

APD DETECTOR PARAMETERS	
QUANTUM EFFICIENCY	η_Q
EFFECTIVE HOLE-TO-ELECTRON IONIZATION RATIO	K_{eff}
AVERAGE DETECTOR GAIN	G
EXCESS NOISE FACTOR	F
GAIN DEPENDENT BULK LEAKAGE CURRENT	I_B
GAIN INDEPENDENT SURFACE LEAKAGE CURRENT	I_S
EQUIVALENT NOISE TEMPERATURE	T_S
LOAD RESISTANCE	R_L

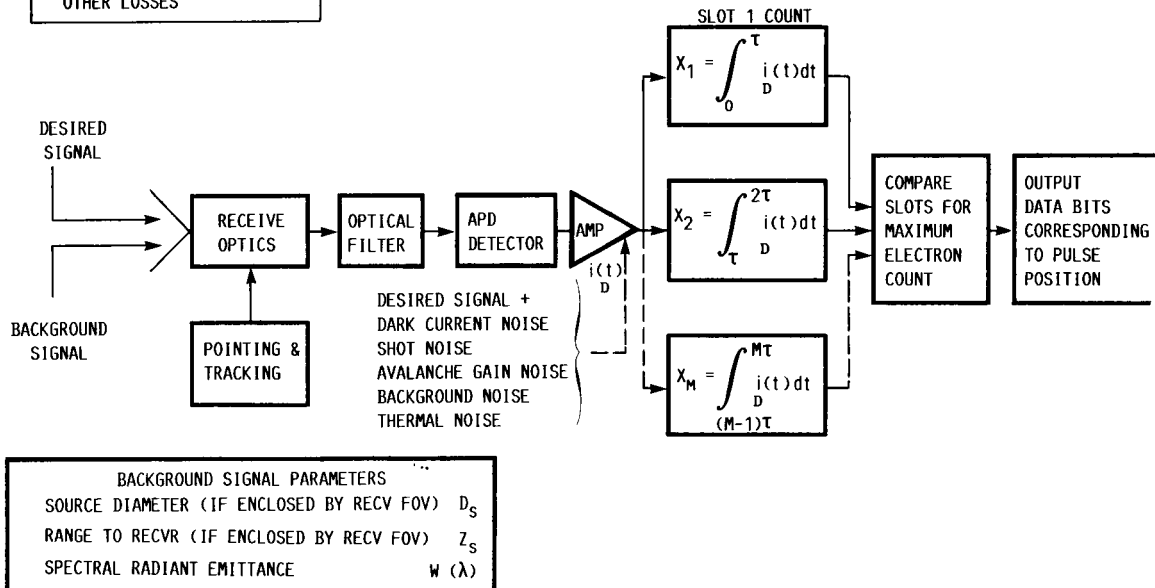


FIGURE 4. - DIRECT DETECTION M-ARY PPM RECEIVER MODEL AND RELEVANT PARAMETERS.

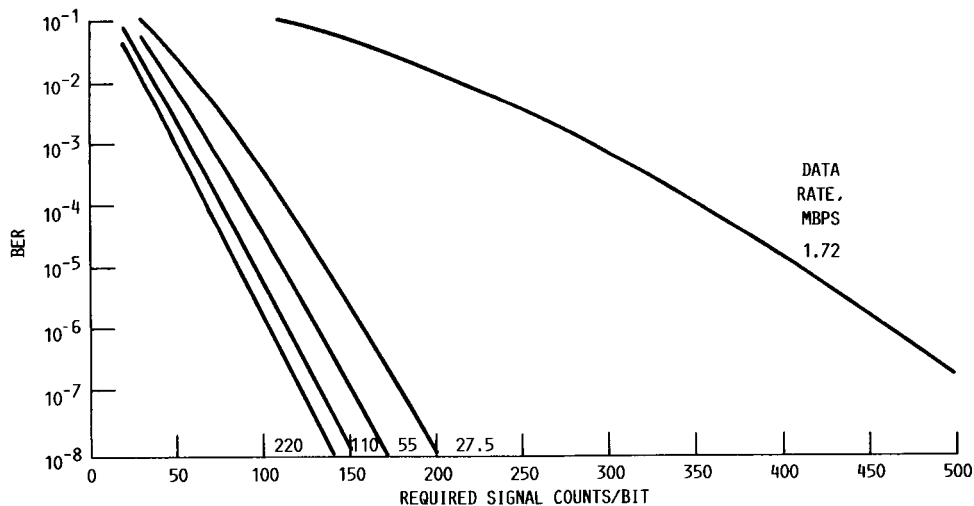


FIGURE 5. - BPPM BER VERSUS REQUIRED SIGNAL COUNTS/BITS. NO BACKGROUND RADIATION SOURCES IN ACTS OR AIRCRAFT RECV FOV. $T_S = 400$ K; $R_L = 2000$ OHMS; EXTINCTION - 5 PERCENT; $G = 150$; $F = 3.5$; $I_S = 10$ nA; $I_B = 0.1$ nA; $Q_E = 0.70$; $N_B = 0$ COUNTS/sec.

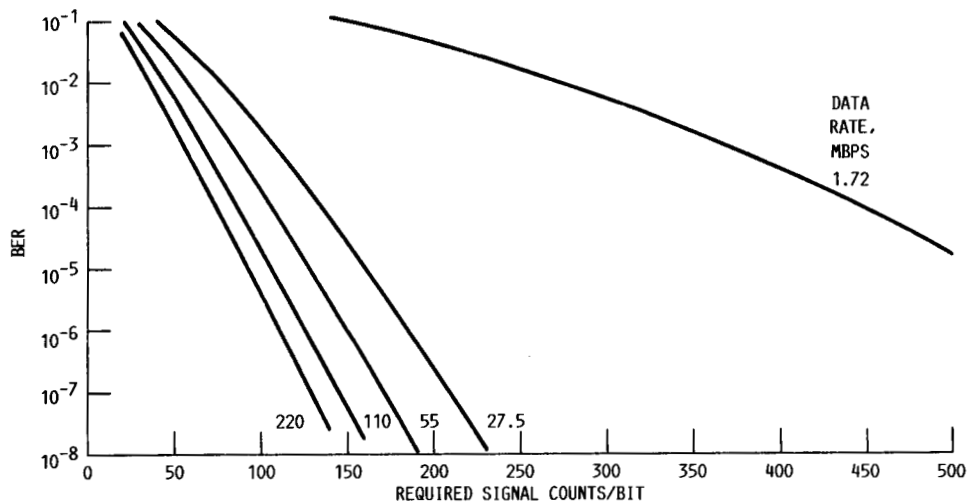


FIGURE 6. - ACTS BPPM BER VERSUS REQUIRED SIGNAL COUNTS/BIT. SUNLIT EARTH IN ACTS RECV FOV. TS = 400 K; RL = 2000 OHMS; EXTINCTION - 5 PERCENT; G = 150; F = 3.5; IS = 10 nA; IB = 0.1 nA; QE = 0.07; NB = 2.2×10^9 COUNTS/SEC.

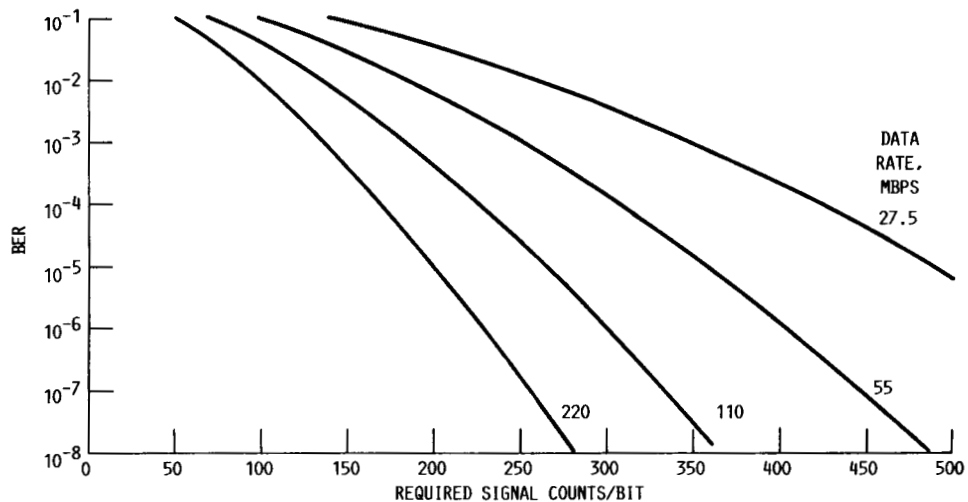


FIGURE 7. - AIRCRAFT BPPM BER VERSUS REQUIRED SIGNAL COUNTS/BIT. SUNLIT SKY IN ACTS RECV FOV. TS = 400 K; RL = 2000 OHMS; EXTINCTION - 5 PERCENT; G = 150; F = 3.5; IS = 10 nA; IB = 0.1 nA; QE = 0.70; NB = 7.6×10^{10} COUNTS/SEC.

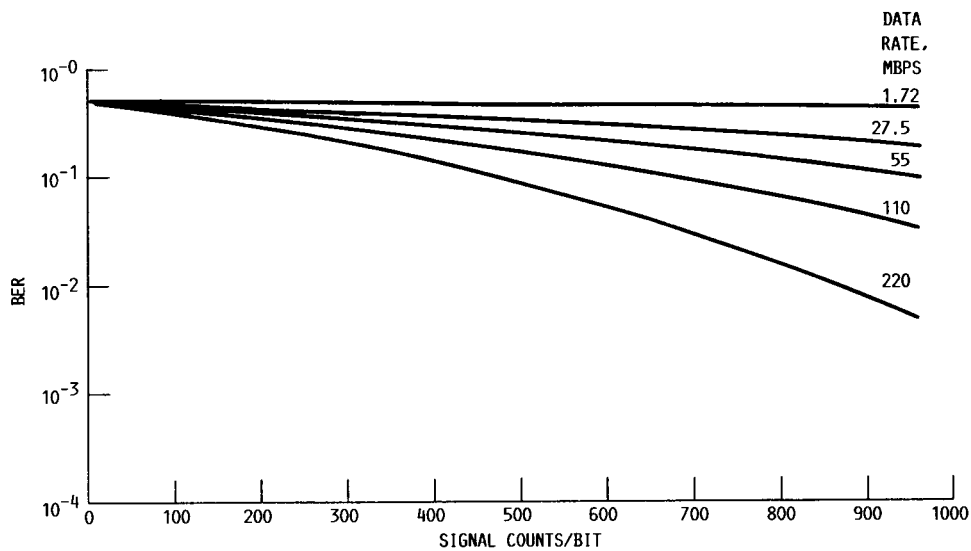


FIGURE 8. - AIRCRAFT BPPM BER VERSUS REQUIRED SIGNAL COUNTS/BITS. SUN IN AIRCRAFT RECV FOV. TS = 400 K; RL = 2000 OHMS; EXTINCTION - 5 PERCENT; G = 150; F = 3.5; IS = 10 nA; IB = 0.1 nA; QE = 0.70; NB = 7.6×10^{12} COUNTS/SEC.

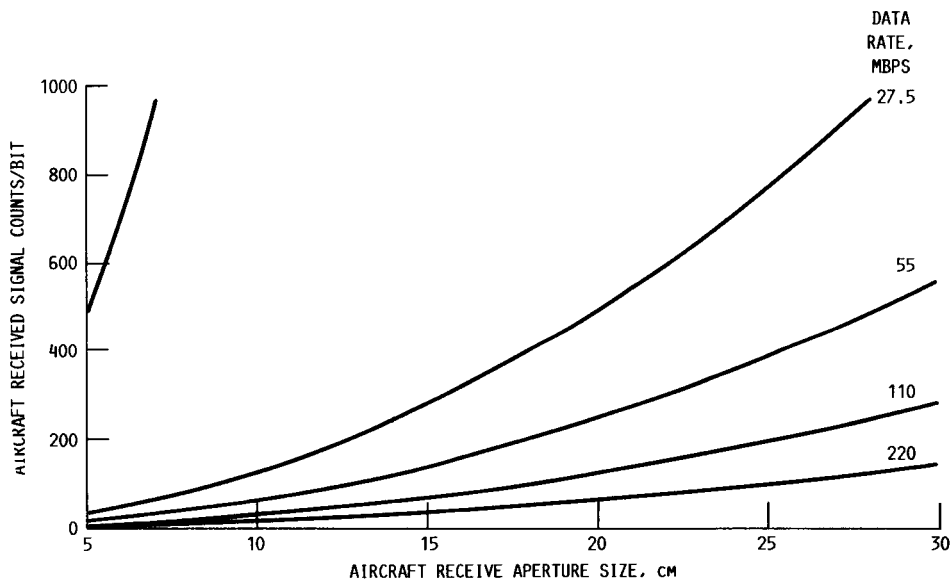


FIGURE 9. - RECV SIGNAL COUNTS/BIT VERSUS AIRCRAFT APERTURE DIAMETER. ACTS-TO-AIRCRAFT COMMUNICATION. $P_t = 30$ MW; XMIT EFF. = 40 PERCENT; $D_t = 20$ cm; POINTING LOSS = 1.02 dB; ATMO LOSS = 0.8 dB; RANGE = 38 070 km; RECV EFF. = 62 PERCENT; QE = 70 PERCENT.

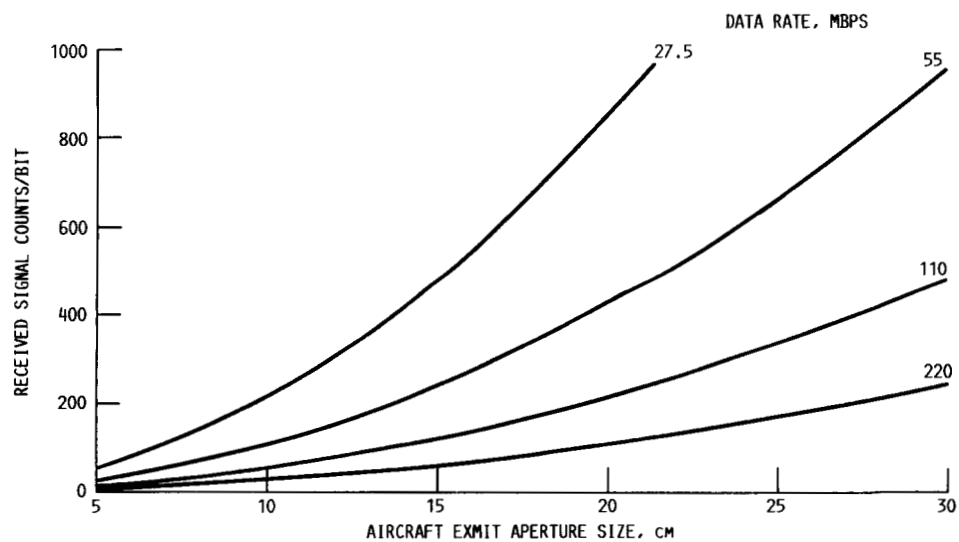


FIGURE 10. - RECV SIGNAL COUNTS/BIT VERSUS AIRCRAFT APERTURE DIAMETER. DATA RATES: 27.5, 55, 110 AND 220 MBPS. AIRCRAFT-TO-ACTS COMMUNICATION. $P_t = 50$ MW; XMIT EFF. = 40 PERCENT $D_r = 20$ cm; POINTING LOSS = -1.02 dB; ATMO LOSS = -0.8 dB; RANGE = 38 070 km; RECV EFF. = 62 PERCENT; QE = 70 PERCENT.



National Aeronautics and
Space Administration

Report Documentation Page

1. Report No. NASA TM-100792		2. Government Accession No.		3. Recipient's Catalog No.	
4. Title and Subtitle A Laser Communication Experiment Utilizing the ACT Satellite and an Airborne Laser Transceiver				5. Report Date	
				6. Performing Organization Code	
7. Author(s) Charles E. Provencher, Jr. and Rodney L. Spence				8. Performing Organization Report No. E-3967	
				10. Work Unit No. 650-60-23	
9. Performing Organization Name and Address National Aeronautics and Space Administration Lewis Research Center Cleveland, Ohio 44135-3191				11. Contract or Grant No.	
				13. Type of Report and Period Covered Technical Memorandum	
12. Sponsoring Agency Name and Address National Aeronautics and Space Administration Washington, D.C. 20546-0001				14. Sponsoring Agency Code	
15. Supplementary Notes Prepared for Optoelectronics and Laser Applications in Science and Engineering (O-E LASE '88) sponsored by the Society of Photo-Optical Instrumentation Engineers, Los Angeles, California, January 10-17, 1988.					
16. Abstract The launch of a laser communication transmitter package into geosynchronous earth orbit onboard the Advanced Communications Technology (ACT) satellite will present an excellent opportunity for the experimental reception of laser communication signals transmitted from a space orbit. The ACTS laser package includes both a heterodyne transmitter (Lincoln Labs design) and a direct detection transmitter (Goddard Space Flight Center design) with both sharing some common optical components. NASA Lewis Research Center's Space Electronics Division is planning to perform a space communication experiment utilizing the GSFC direct detection laser transceiver. The laser receiver will be installed within an aircraft provided with a glass port for the reception of the signal. This paper describes the experiment and the approach to performing such an experiment. Described are the constraints placed upon the NASA Lewis experiment by the performance parameters of the laser transmitter and by the ACTS spacecraft operations. The conceptual design of the receiving terminal is given; also included is the anticipated performance capability of the detector.					
17. Key Words (Suggested by Author(s)) Direct detection laser; Satellite to aircraft communications; Pulse position modulation; Optical receiver sensitivity				18. Distribution Statement Unclassified - Unlimited Subject Category 36	
19. Security Classif. (of this report) Unclassified		20. Security Classif. (of this page) Unclassified		21. No of pages 26	22. Price* A03